40. Schwartz RH. Costimulation of T lymphocytes: the role of CD28, CTLA-4, and B7/BB1 in interleukin-2 production and immunotherapy. Cell **1992**; 71:1065–8.
41. Garrity PA, Chen D, Rothenberg EV, Wold BJ. Interleukin-2 transcription is regulated in vivo at the level of coordinated binding of both constitutive and regulated factors. Mol Cell Biol **1994**; 14: 2159–69.
42. Sanchez-Lockhart M, Marin E, Graf B, et al. Cutting edge: CD28-mediated transcriptional and posttranscriptional regulation of IL-2 expression are controlled through different signaling pathways. J Immunol **2004**; 173:7120–4.
43. Zanussi S, Simonelli C, D'Andrea M, et al. CD8+ lymphocyte phenotype and cytokine production in long-term non-progressor and in progressor patients with HIV-1 infection. Clin Exp Immunol **1996**; 105:220–4.

PLOS | ONE

Development and Customization of a Color-Coded Microbeads-Based Assay for Drug Resistance in HIV-1 Reverse Transcriptase

Lijun Gu[1,2], Ai Kawana-Tachikawa[3], Teiichiro Shiino[4], Hitomi Nakamura[5,6], Michiko Koga[3,6], Tadashi Kikuchi[3,6], Eisuke Adachi[6], Tomohiko Koibuchi[6], Takaomi Ishida[1,2], George F. Gao[7], Masaki Matsushita[8], Wataru Sugiura[4], Aikichi Iwamoto[1,3,5,6], Noriaki Hosoya[3,5]*

1 Research Center for Asian Infectious Diseases, the Institute of Medical Science, the University of Tokyo, Tokyo, Japan, **2** Japan-China Joint Laboratory of Molecular Immunology and Molecular Microbiology, Institute of Microbiology, Chinese Academy of Sciences, Beijing, P. R. China, **3** Division of Infectious Diseases, Advanced Clinical Research Center, the Institute of Medical Science, the University of Tokyo, Tokyo, Japan, **4** AIDS Research Center, National Institute of Infectious Diseases, Tokyo, Japan, **5** Department of Infectious Disease Control, International Research Center for Infectious Diseases, the Institute of Medical Science, the University of Tokyo, Tokyo, Japan, **6** Division of Infectious Diseases and Applied Immunology, Research Hospital, The Institute of Medical Science, The University of Tokyo, Tokyo, Japan, **7** CAS Key Laboratory of Pathogenic Microbiology and Immunology, Institute of Microbiology, Chinese Academy of Sciences, Beijing, P. R. China, **8** Biotech Research and Development, Wakunaga Pharmaceutical Corporation, Hiroshima, Japan

Abstract

Background: Drug resistance (DR) of HIV-1 can be examined genotypically or phenotypically. Although sequencing is the gold standard of the genotypic resistance testing (GRT), high-throughput GRT targeted to the codons responsible for DR may be more appropriate for epidemiological studies and public health research.

Methods: We used a Japanese database to design and synthesize sequence-specific oligonucleotide probes (SSOP) for the detection of wild-type sequences and 6 DR mutations in the clade B HIV-1 reverse transcriptase region. We coupled SSOP to microbeads of the Luminex 100 xMAP system and developed a GRT based on the polymerase chain reaction (PCR)-SSOP-Luminex method.

Results: Sixteen oligoprobes for discriminating DR mutations from wild-type sequences at 6 loci were designed and synthesized, and their sensitivity and specificity were confirmed using isogenic plasmids. The PCR-SSOP-Luminex DR assay was then compared to direct sequencing using 74 plasma specimens from treatment-naïve patients or those on failing treatment. In the majority of specimens, the results of the PCR-SSOP-Luminex DR assay were concordant with sequencing results: 62/74 (83.8%) for M41, 43/74 (58.1%) for K65, 70/74 (94.6%) for K70, 55/73 (75.3%) for K103, 63/73 (86.3%) for M184 and 68/73 (93.2%) for T215. There were a number of specimens without any positive signals, especially for K65. The nucleotide position of A2723G, A2747G and C2750T were frequent polymorphisms for the wild-type amino acids K65, K66 and D67, respectively, and 14 specimens had the D67N mutation encoded by G2748A. We synthesized 14 additional oligoprobes for K65, and the sensitivity for K65 loci improved from 43/74 (58.1%) to 68/74 (91.9%).

Conclusions: We developed a rapid high-throughput assay for clade B HIV-1 DR mutations, which could be customized by synthesizing oligoprobes suitable for the circulating viruses. The assay could be a useful tool especially for public health research in both resource-rich and resource-limited settings.

Citation: Gu L, Kawana-Tachikawa A, Shiino T, Nakamura H, Koga M, et al. (2014) Development and Customization of a Color-Coded Microbeads-Based Assay for Drug Resistance in HIV-1 Reverse Transcriptase. PLoS ONE 9(10): e109823. doi:10.1371/journal.pone.0109823

Editor: Nicolas Sluis-Cremer, University of Pittsburgh, United States of America

Received May 7, 2014; **Accepted** September 10, 2014; **Published** October 14, 2014

Data Availability: The authors confirm that all data underlying the findings are fully available without restriction. All relevant data are within the paper.

Funding: This work was supported in part by a contract research fund from the Ministry of Education, Culture, Sports, Science and Technology (MEXT) for Program of Japan Initiative for Global Research Network on Infectious Diseases (10005010)(AI); Global COE Program (Center of Education and Research for Advanced Genome-Based Medicine - For personalized medicine and the control of worldwide infectious diseases -) of MEXT (F06)(AI); JSPS KAKENHI (25293226)(AKT); JSPS KAKENHI (24790437, 26860300)(NH);Grants for AIDS research from the Ministry of Health, Labor, and Welfare of Japan (H24-AIDS-IPPAN-008)(AKT); Grants for AIDS research from the Ministry of Health, Labor, and Welfare of Japan (H25-AIDS-IPPAN-006)(NH); Research on international cooperation in medical science, Research on global health issues, Health and Labour Science Research Grants, the Ministry of Health, Labor, and Welfare of Japan (H25-KOKUI-SITEI-001)(AI). The funders had no role in study design, data collection and analysis, decision to publish, or preparation of the manuscript.

Competing Interests: A.I. has received grant support from Toyama Chemical Co. Ltd., astellas, ViiV Healthcare K.K., MSD K.K., Baxter through the University of Tokyo. A.I. has received speaker's honoraria/payment for manuscript from Eiken Chemical Co. Ltd., astellas, Toyama Chemical Co. Ltd, Torii Pharmaceutical Co. Ltd., Takeda Pharmaceutical Co. Ltd. and MSD. MM is an employee of Wakunaga Pharmaceutical Corporation which keeps a patent on PCR amplification sequence-specific oligonucleotide probes (SSOP) method. For the remaining authors none were declared. This does not alter the authors' adherence to PLOS ONE policies on sharing data and materials.

* Email: hnori@ims.u-tokyo.ac.jp

Introduction

Since combination antiretroviral therapy (cART) was introduced, the prognosis of patients with HIV-1 infection has improved dramatically [1,2]. In resource-rich settings, new classes, new drugs or new formulations of previously-known classes of antiretroviral drugs (ARV) have been introduced continuously for clinical use. Nucleoside/nucleotide reverse transcriptase inhibitor (NRTI) resistance has declined over time in resource-rich settings, presumably reflecting the improvement of treatment regimens [3,4]. Rates of transmitted HIV-1 drug resistance (DR) have remained limited also in resource-limited settings; however, limitation of the first-line and subsequent regimens would be a concern. cART consisting of two NRTIs and one non-nucleoside reverse transcriptase inhibitors (NNRTI), most often zidovudine (AZT) + lamivudine (3TC) or stavudine (d4T) + 3TC plus nevirapine (NVP) or efavirenz (EFV), has been widely used as the treatment regimen in the resource-limited settings [5,6]; consequently, DR might become a larger public health challenge in the developing countries.

DR can be examined genotypically or phenotypically [7] (http://www.aidsmap.com/pdf/Resistance-tests/page/1044559/). Although sequencing is the gold standard of the genotypic resistance testing (GRT), high-throughput GRT targeted to the codons responsible for DR may be more convenient and suitable for public health research [8,9]. We applied the PCR-SSOP-Luminex method [10–12] to an HIV-1 GRT. As an initial approach, we focused on designing an assay for six major DR mutations: M41L, K65R, K70R, K103N, M184V and T215Y/F. M41L, K70R, T215F/Y are examples of thymidine analogue mutations (TAMs) and associated with AZT and d4T [13] (HIV Drug resistance database, Stanford University, http://hivdb.stanford.edu/index.html). K65R is associated multi-nucleoside and nucleotide DR. Although K65R is selected by nucleotide reverse transcriptase inhibitor tenofovir (TDF) usually, it can be selected by d4T. K103N is highly associated with EFV and NVP resistance. The K103N mutation reduces susceptibility to NVP by 50-flod, and EFV by 20-fold. M184V is highly associated with 3TC and emtricitabine (FTC) resistance, and reduce the susceptibility to 3TC by 200-fold. The monitoring of these six DR mutations should be important for molecular epidemiologic study estimating the efficacy of anti-HIV drugs especially in resource limited settings. We synthesized the oligonucleotides for the primers and probes based on the Japanese data base on reverse transcriptase mutations. In order to validate the initial assay system and examine the flexibility for customization, we focused on the clade B HIV-1 which is most prevalent in Japan. Here we report the results of the comparison between sequencing and the PCR-SSOP-Luminex assay using the specimens of a Japanese cohort.

Methods

PCR-SSOP-Luminex assay

HIV-1 DR genotyping described here is based on the reverse SSOP method coupled with a microsphere beads array platform (Luminex Corporation, Austin, TX, USA). Briefly, the method involves PCR amplification by biotinylated primers, hybridization to nucleotide probes coupled to microbeads, detection of the bound PCR products by streptavidin-phycoerythrin (SAPE) reaction, and quantitation by measurement of median fluorescence intensity (MFI).

Color-coded microbeads were coupled to oligoprobes derived from DR mutations or conserved sequences in HIV-1 RT coding region. These synthesized probes were modified at the 5′-end with a terminal amino group and covalently bound to the carboxylated fluorescent microbeads using ethylene dichloride (EDC), following the procedures recommended by the manufacturer (Wakunaga Pharmaceutical Co. Ltd, Hiroshima, Japan). Briefly, 6.25×10^5 carboxylated microbeads were suspended in 50 μl of 0.1 M MES (2-(N-morpholino) ethane sulfonic acid, pH 4.5 (Dojindo Laboratories, Kumamoto Techno Research Park, Kumamoto, Japan). Afterwards, 0.5 μM of amine-substituted oligonucleotide probes was added, followed by 100 mg/ml EDC (1-Ethyl-3-(3-dimethylaminopropyl) carbodiimido hydrochloride) (Pierce Biotechnology, Rockford, IL, USA), and the mixture was incubated in the dark for 30 min at 25°C. The EDC addition and incubation were repeated twice and the microbeads were washed once with 0.02% Tween-20 and once with 0.1% SDS. After the final wash, the pellets were resuspended in 50 μl TE buffer (pH 8.0), and counted on a hemocytometer. The concentration of fluorescence-labeled microbeads coupled to oligonucleotide probes (oligobeads) was adjusted to 8000–12000/μl, and oligobeads were stored at 4°C in the dark.

Five-microliter aliquots of the 5′-biotinlabeled amplified DNA were added to wells in a 96-well PCR tray containing 5 μl/well of denaturation solution, and allowed to denature for 5 min at RT. Hybridization mixture was prepared using oligobeads stocks, SAPE and hybridization solution, according to the manufacturer's instructions (Wakunaga Pharmaceutical Co. Ltd, Hiroshima, Japan). Twenty-five-microliter aliquots of hybridization mixture containing 500 each sequence-specific oligobeads were added to each well. The amplicons were hybridized at 55°C for 30 min using the thermal cycler. Hybridized amplicons were washed twice with 75 μl of wash solution in each well. Reaction outcomes were measured by the Luminex 100 flow cytometer that is equipped with two types of lasers. The bead populations were detected and identified using the 635 nm laser. The SAPE fluorescence of the biotin labeled amplicons that had hybridized to the oligobeads was quantitated using the 532 nm laser. The MFI of SAPE was used to quantify the amount of DNA bound to the oligobeads. Assays were performed in triplicate.

Site-directed mutagenesis and plasmid construction

To assess the feasibility of the assay system, we chose cloned SF2 genome (GenBank accession number K02007) as a template. Synthesized PCR fragments with DR mutations created by site-directed mutagenesis were inserted into the SF2 genome. The numbering system used to refer to DR mutations was based on HXB2 genome (HXB2 location 2485–3309, GenBank accession number K03455) sequences. The SF2 and HXB2 genome had the same sequence in the regions covered by the probes.

Plasmid p9B/R7 from the HIV-1 SF2 strain was a kind gift of Dr. T. Shioda (Osaka University, Osaka, Japan) [14,15]. An *Xho* I- *BamH* I fragment including the pol gene from p9B/R7 was subcloned into pBluescript II SK (+) (Stratagene, La Jolla, CA, USA). As shown in Fig. 1A, various DR mutations were introduced into the *Xho* I- *BamH* I fragment of the plasmid by site-directed mutagenesis using oligonucleotides and PCR methods as previously described [16], and were confirmed by sequencing.

Clinical specimens

Sixty subjects were selected from among patients participating in an ongoing study on microbes at an HIV outpatient clinic affiliated with the Institute of Medical Science, the University of Tokyo (IMSUT). The study was approved by the internal review board of IMSUT (20-31-1120), and all subjects provided written informed consent. The median HIV-1 RNA and CD4 cells count

A

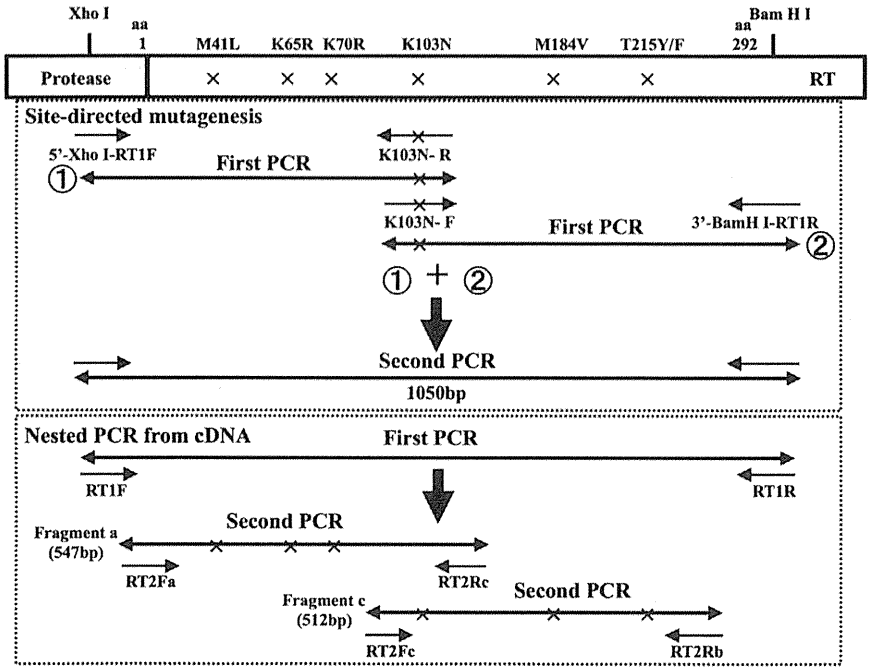

B

PCR primers

RT1F: 5'-ATGATAGGGGGAATTGGAGGTTT- 3'

RT1R: 5'- TACTTCTGTTAGTGCTTTGGTTCC- 3'

RT2Fa: 5'- GACCTACACCTGTCAACATAATTGG- 3'

RT2Rc: 5'- TGGAATATTGCTGGTGATCC- 3'

RT2Fc: 5'-AACTCAAGACTTCTGGGAAGT- 3'

RT2Rb: 5'-CAGTCCAGCTGTCTTTTTCTGGC- 3'

Sequencing primers

T7: 5'-TAATACGACTCACTATAGGG-3'

Rev: 5'-CAGGAAACAGCTATGAC-3'

Figure 1. Schematic representation of PCR amplification and sequences of primers for PCR and sequencing. (A) Top: Site-directed mutagenesis using oligonucleotide is shown using K103N as an example. Desired mutations in the reverse transcriptase gene were engineered in two PCR fragments, then incorporated into a larger fragment (1050 bp, HXB2 location 2388–3425) by the second PCR, and cloned into pBluescript II SK (+) at *XhoI-BamHI* sites. Bottom: Negative strand cDNA was synthesized from patients' plasma. After the first strand PCR using RT1F and RT1R as primers, Fragment a or Fragment c were amplified by nested PCR. (B) Primer sequences for PCR amplification and sequencing.
doi:10.1371/journal.pone.0109823.g001

at sampling were 4.15 (range 2.60–5.88) log 10 copies/ml and 264 (range: 9–902) cells/μl, respectively. Seventy-four specimens from 60 patients were analyzed in this study. Forty-eight patients contributed one plasma specimen, 10 patients contributed two plasma specimens from different time points, and two patients contributed three separate plasma specimens. Twenty-two specimens were from patients who were treatment-naïve when the plasma specimens were obtained. The remaining 52 specimens were from patients on failing treatment including NRTI at the time of sample collection.

Viral RNA extraction, cDNA synthesis, and PCR amplification

Viral RNA was extracted from 140 μl plasma using QIAamp Viral RNA Mini Kit (QIAGEN, Valencia, CA, USA) and eluted

Table 1. Design of oligoprobes based on clade B HIV-1 sequences from Japanese surveillance database.

Locus	genetic code	Frequency(%)	Name of probe	Oligoprobes	Nucleotide sequence (5'-3')	100% match isolates of database
M41					TGT ACA GAA ATG GAA	
	M41-ATG	795/795(100)	M41M-ATG	GTACAGAAATGGAA	— — — — —	618/868(71.2%)
	M41L-TTG	109/180(60.6)	M41L-TTG	GTACAGAATTGGAA	— — — T— —	
	M41L-CTG	69/180(38.3)	M41L-CTG	GTACAGAACTGGAA	— — — C— —	
	M41L-TTA	1/180(0.6)				
	M41L-TTR	1/180(0.6)				
K65					ATA AAG AAA AAA GAC AGT	
	K65-AAA	961/1012(95.0)	K65K-AAA	ATAAAGAAAAAAGACAG	— — — — — —	516/870(59.3%)
	K65-AAG	30/1012(3.0)				
	K65-AAR	21/1012(2.1)				
	K65R-AGA	7/7(100)	K65R-AGA	ATAAAGAGAAAAGACAG	— — -G- — — —	
	K65R-AGG	0/7(0.0)				
K70					GAC AGT ACT AAA TGG AGA	
	K70-AAA	849/885(95.9)	K70K-AAA-1	GACAGTACTAAATG	— — — — —	621/769(80.8%)
			K70K-AAA-2	GTACTAAATGGAGA	— — — — — —	
	K70-AAG	17/885(1.9)				
	K70-AAR	19/885(2.1)				
	K70R-AGA	85/88(96.6)	K70R-AGA	GTACTAGATGGAGA	— — -G- — —	
	K70R-AGG	0/88(0.0)	K70R-AGG	GTACTAGGTGGAGA	— — -GG — —	
	K70R-AGR	3/88(3.4)				
K103					TTA AAA AAG AAA AAA TCA GTA	
	K103-AAA	815/867(94.0)	K103K-AAA	AAAAAAGAAAAAATCAG	- — — — — — — -	558/785(71.1%)
	K103-AAG	25/867(2.9)				
	K103-AAR	27/867(3.1)				
	K103N-AAC	112/128(87.5)	K103N-AAC	AAAAAAGAACAAATCAG	- — — —C — — -	
	K103N-AAT	3/128(2.3)	K103N-AAT	AAAAAAGAATAAATCAGT	- — — —T — — —	
	K103N-AAY	13/128(10.2)				
M184					TAT CAA TAC ATG GAT GAT	
	M184-ATG	659/659(100)	M184M-ATG	TATCAATACATGGATG	— — — — — -	761/888(85.7%)
	M184V-GTG	295/335(88.1)	M184V-GTG	TATCAATACGTGGATG	— — — G— — -	
	M184V-GTA	14/335(4.2)				
	M184V-GTR	26/335(7.8)				
T215					TGG GGA TTT ACC ACA CCA	
	T215-ACC	692/724(95.6)	T215T-ACC-1	GGGGATTTACCACA	— — — — —	583/813(71.7%)
			T215T-ACC-2	GGGGATTTACCACACCA	— — — — — —	
	T215-ACT	13/724(1.8)				
	T215-ACA	7/724(1.0)				
	T215-ACG	3/724(0.4)				
	T215-ACY	8/724(1.1)				
	T215-ACM	1/724(0.1)				
	T215F-TTC	54/54(100)	T215F-TTC	GGGGATTTTTCACAC	— — — TT- —	
	T215Y-TAC	182/185(98.4)	T215Y-TAC	GGGGATTTTACACAC	— — — TA- — -	
	T215Y-TAT	2/185(1.1)				
	T215Y-TAY	1/185(0.5)				
Standard probes			S2582	ATTAAAGCCAGGAATGGAT		
			S2693	AAAAATTGGGCCTGAAAAT		
			S3230	CCTTTGGATGGGTTATGAA		
			S3252	CATCCTGATAAATGGACAG		

Table 1. Cont.

Locus	genetic code	Frequency(%)	Name of probe	Oligoprobes	Nucleotide sequence (5′-3′)	100% match isolates of database
			S3243	TATGAACTCCATCCTGA		

R: Mixed base of A and G; Y: Mixed base of C and T; M: Mixed base of C and A.
doi:10.1371/journal.pone.0109823.t001

with 60 μl AVE buffer. For cDNA synthesis, 55 μl of RNA solution was mixed with 5 μl of 100 pmol/μl random primer (TaKaRa Bio, Otsu, Shiga, Japan) or specific primer, RT1R (Fig. 1B), and 5 μl of 10 mM dNTPs, and denatured at 70°C for 10 min. The RT mixture containing 20 μl of 5× First-Strand buffer, 5 μl of 0.1 M DTT, 5 μl of RNaseOUT Recombinant RNase inhibitor (40 U/μl; Invitrogen, Carlsbad, California, USA) and 5 μl of SuperScript III RT (200 U/μl, Invitrogen) was added to the 65 μl denatured viral RNA-primer-dNTP mixture. The reaction mixture (100 μl final volume) was incubated at 25°C for 5 min for annealing and then at 55°C for 60 min for reverse transcription. The reaction was inactivated by heating at 70°C for 15 min.

RT gene fragments were amplified by nested PCR from cDNAs or by single PCR from plasmids. For the first reaction a 1050 bp fragment from the RT coding region was amplified from 5 μl aliquots of cDNAs using RT1F and RT1R as outer primers in a reaction mixture containing 50 μl of 1×Prime STAR buffer, 0.2 mM of each dNTPs, 0.5 μM of each primer, and 0.5 μl Prime STAR HS DNA Polymerase (25 U/μl, TaKaRa Bio, Otsu, Shiga, Japan). Amplification conditions consisted of 35 cycles denaturation at 98°C for 10 s, annealing at 55°C for 5 s, and extension at 72°C for 30 s.

For the second reaction of the nested PCR and for the single PCR from plasmids (0.1 pg), RT coding fragments were amplified in two PCR fragments using two 5′ biotinylated primer sets, PS1 and PS2, as described previously [17]. The PS1 primer set produced a 547 bp amplicon that was used to detect M41L, K65R, K70R, and K103N, and the PS2 primer set produced a 512 bp amplicon that was used to detect K103N, M184V, and T215Y/F (Fig. 1A). The reaction mixture used 5 μl of the first PCR products or 0.1 pg of plasmid DNA in a final volume of 50 μl, as described above, with amplification conditions as follows: 25 cycles (second nested PCR) or 35 cycles (plasmid DNA amplification) of denaturation at 98°C for 10 s, annealing at 55°C for 5 s, and extension at 72°C for 1 min. The PCR amplicons were used for Luminex detection or direct sequencing.

Sequencing

PCR products were purified with the QIAquick PCR Purification Kit (QIAGEN, Valencia, CA, USA) and were directly sequenced in both directions using ABI 3130xl genetic analyzer (Applied Biosystems, Foster City, CA, USA) and Big Dye terminator V3.1 cycle sequencing kit (Applied Biosystems). In the case of sequence ambiguity due to a coexistence of multiple nucleotides, we confirmed the sequence by cloning and sequencing. For cloning and sequencing, the purified PCR fragments were phosphorylated using T4 polynucleotide kinase (TaKaRa Bio, Otsu, Shiga, Japan) and inserted into the dephosphorylated *EcoR*V restriction site of pBluescript II SK(+). Inserts were sequenced using T7 and Rev universal primers (Fig. 1B).

HIV-1 Japanese surveillance database

In Japan 10 university hospitals, 5 medical centers, 5 public health laboratories, and the National Institute of Infectious Diseases are collaborating in the surveillance of newly diagnosed HIV/AIDS cases. HIV/AIDS patients with both acute and chronic infections, newly diagnosed at these centers since January 2003 were enrolled [18]. Prevalence of DR codons in these patients was determined by analysis of sequences of clade B HIV-1 reverse transcriptase positions 1–240 amino acids.

Statistical analysis

GraphPad Prism 5.0 software (GraphPad Software Inc., San Diego, CA) was used for statistical data analysis. Statistical significance was defined as $P<0.05$.

Results

Design of oligoprobes based on the database of clade B HIV-1 sequences in Japan

Based on the frequency of the codon usage in the Japanese surveillance database for amino acids M41, K65, K70, K103, M184 and T215 in RT gene, we designed the nucleotide sequence of 18 oligoprobes for DR mutation and 5 standard probes (Table 1). We adopted nucleotide sequences of HXB2 strain for the flanking sequences. Synthesized oligoprobes could cover 71.2%, 59.3%, 80.8%, 71.1%, 85.7% and 71.7% of M41, K65, K70, K103, M184 and T215, respectively (Table 1). Five standard probes were designed in the conserved region of RT gene and used as the assay control.

Evaluation of PCR-SSOP-Luminex DR assay using cloned HIV-1

We examined the sensitivity and specificity of the PCR-SSOP-Luminex DR assay using cloned HIV-1. The test fragments were amplified (Fig. 2A), and the amplicons were hybridized to the 16 oligobeads. We performed three independent assays with triplicate hybridization and detection in each assay. The mean positive signal and standard deviation were 5237±1398 (Fig. 2B). The CV% of positive signal and standard deviation were 10.1% ±10.7. The mean of negative signal and standard deviation were 131.2±69.4. The CV% of negative signal and standard deviation were 21.6±23.6 (mean ± S.D.). MFIs of hybridization signals were clearly high only when the oligoprobes matched the mutations in the fragments (Fig. 2B). These data confirmed that the assay system could discriminate one base mismatch at M41, K65, K70, K103, M184 and T215 codons in the plasmid-probe model system.

Next, we examined the sensitivity to detect a particular sequence in a mixture for each DR-related site. The plasmids carrying the wild type and mutant sequences were mixed at various ratios. In samples containing only the wild type sequences, the mean background signal (% ±2SD) was 2.0% ±1.2, 4.1%

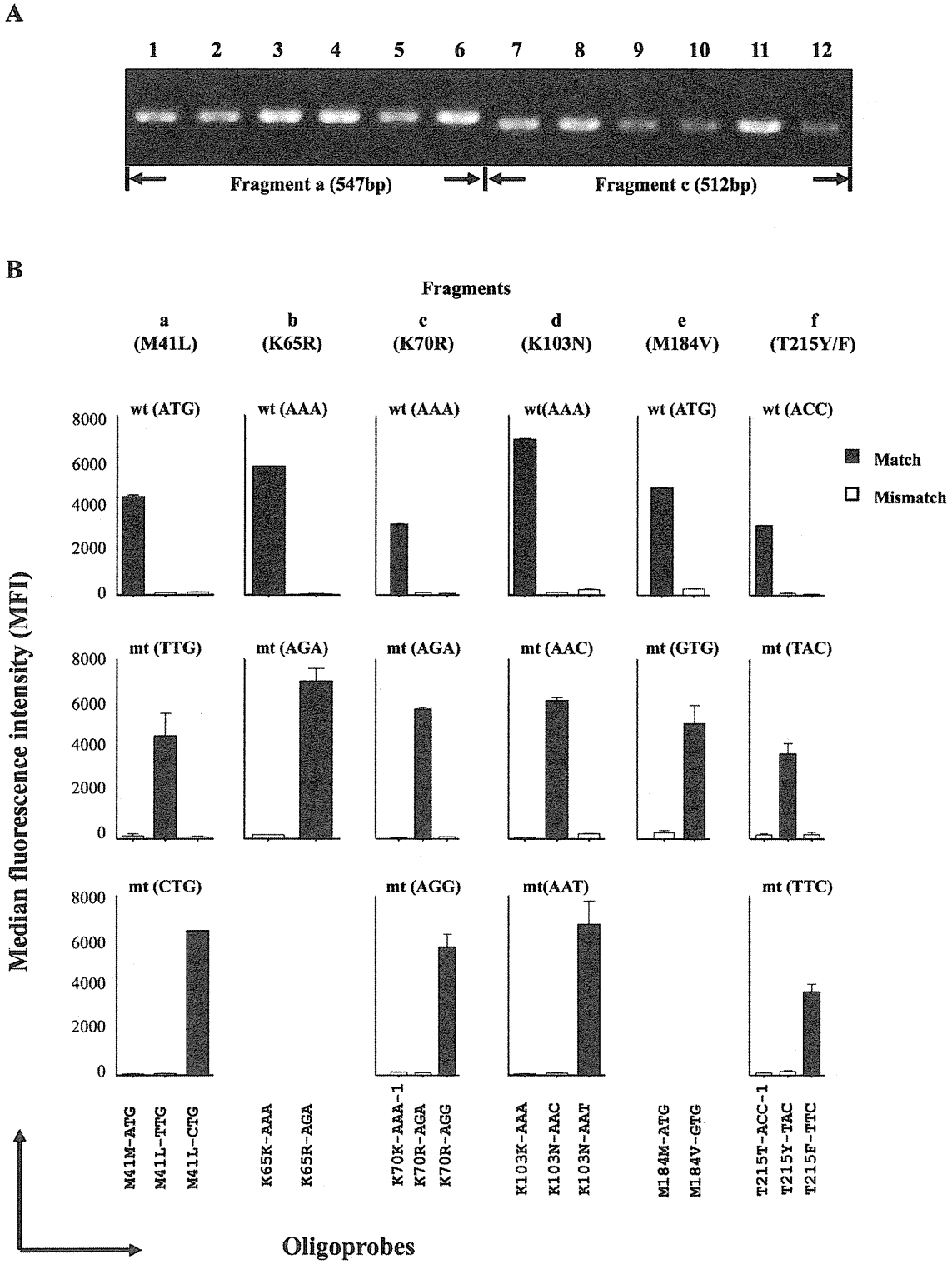

Figure 2. Validation of PCR-SSOP-Luminex assay using plasmids as templates. (A) Agarose gel electrophoresis of amplified fragments. Lanes 1–6: Fragment a (547 bp). Lanes 7–14: Fragment c (512 bp). 1, wild type; 2, M41L-TTG; 3, M41L-CTG; 4, K65R-AGA; 5, 70R-AGA; 6, 70R-AGG; 7, wild type; 8, 103N-AAC; 9, K103N-AAT; 10, M184V-GTG; 11, T215Y-TAC; 12, T215F-TTC. (B) Median fluorescence intensities (MFIs). The plasmid in the test sample is indicated on the top of each panel. Oligoprobes used for detection are indicated at the bottom. Matched results are shown as black bars, mismatched results as white bars. Assays were performed in triplicate. The mean ± standard deviation is shown at the top of each bar.
doi:10.1371/journal.pone.0109823.g002

±2.6, 3.3% ±1.2, 4.6% ±1.8, 6.2% ±3.2 and 3.3% ±0.4 at M41, K65, K70, K103, M184 and T215, respectively (Fig. 3B). The signal for the mutant was judged positive when "% signal" from the mutant oligobeads exceeded the mean + 2SD; 3.2%,

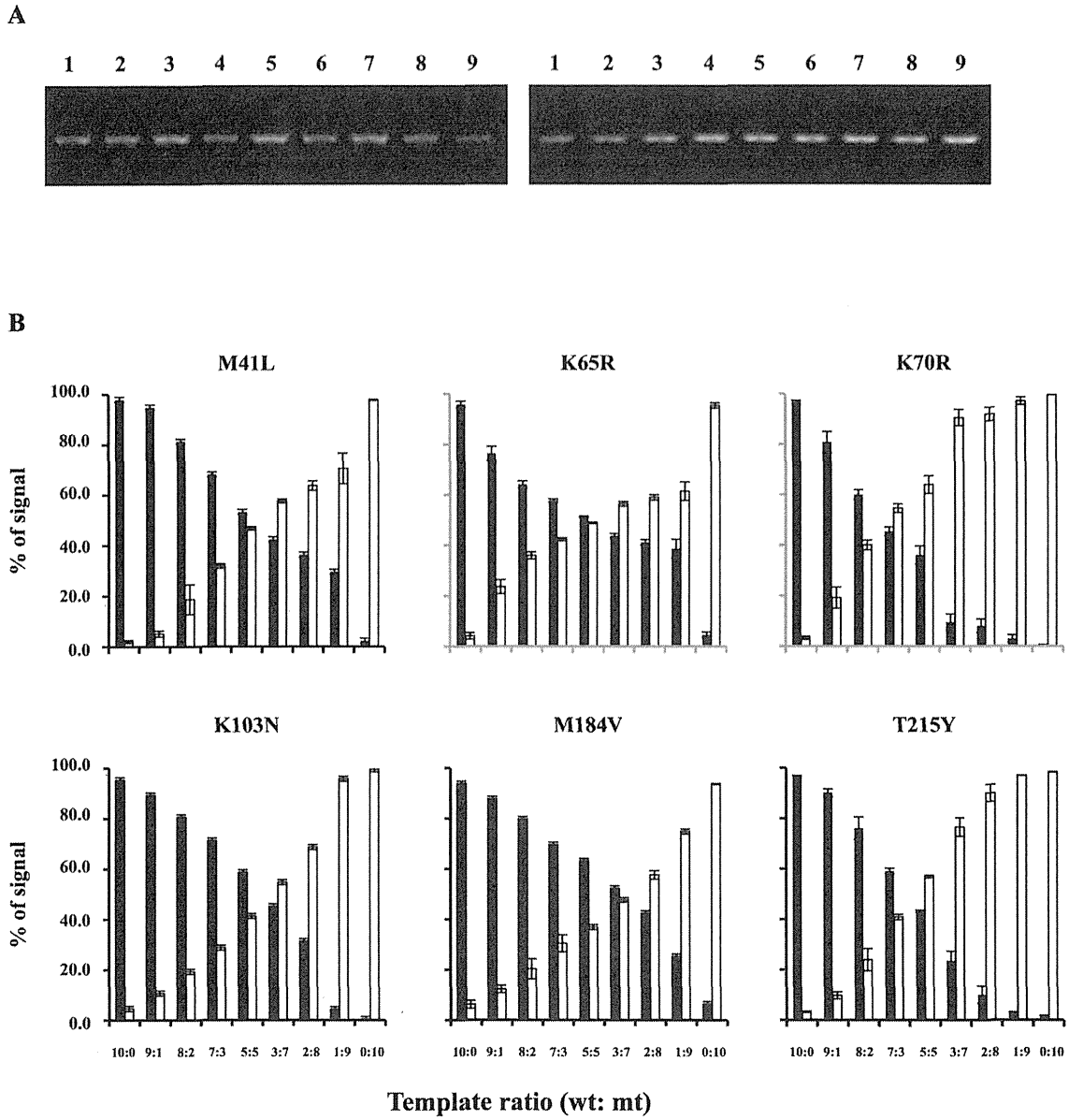

Figure 3. Assay sensitivity in a mixture. (A) Agarose gel electrophoresis of mixtures of amplified fragments. Left panel: Fragment a (547 bp). Right panel: Fragment c (512 bp). Wild-type:mutant ratio; Lanes 1 (10:0); 2 (9:1); 3 (8:2); 4 (7:3); 5 (5:5); 6 (3:7); 7 (2:8); 8 (1:9); 9 (0:10). (B) Signals from wild type probes (black bars) and mutant probes (white bars) in each mixture. "% of signal" was calculated by "MFI of wild type or mutant signal" divided by "MFI of wild type plus mutant signal" and multiplied by 100. Triplicate experiments were performed three times. "% of signal" is shown with standard deviations.
doi:10.1371/journal.pone.0109823.g003

6.7%, 4.5%, 6.4%, 9.4%, 3.7% at M41, K65, K70, K103, M184 and T215, respectively. Actual signals from the mutant oligoprobes at 9:1 (wild type:mutant) mixture at these sites was 5.1%, 23.6%, 19.2%, 10.7%, 12.3%, 9.8%, respectively. Therefore, we infer that the assay can detect 10% DR mutants in the population. There was a big variation (5.1 to 23.6%) in detection of 10% mixtures. We suppose that the difference in minor variant detection could be caused by the melting temperature (GC content and length). Although we compared the GC content and probe length, we could not find a reasonable explanation from this list (data not shown).

Identification of DR mutations in clinical specimens by sequencing

In order to determine the sequence, we amplified the RT gene in two separate fragments from frozen plasma (Fig. 1A). We succeeded to amplify fragment a (containing M41, K65, K70) from all 74 specimens, but failed to amplify fragment c (containing K103, M184, T215) in one patient. Infection with clade B HIV-1 was confirmed by phylogenetic analysis of the RT gene. DR mutations were found at codons M41L (n = 22), K65R (n = 3), K70R (n = 10), K103N (n = 7), M184V (n = 21) and T215Y/F (n = 22) in 40 specimens (Table 2).

Table 2. Comparison of the results between sequencing and PCR-SSOP-Luminex assay.

Position	Aminoacid	Codons	Number of specimens (percentage)	
			Direct sequencing	PCR-SSOP-Luminex
41	Met	ATG	52 (70.3)	41 (55.4)
	Leu	TTG	16 (21.6)	16 (21.6)
		CTG	5 (6.8)	5 (6.8)
	Met, Leu mix		1 (1.4)	0
	No reaction		-	12 (16.2)
65	Lys	AAA	64 (86.5)	41 (55.4)
		AAG	4 (5.4)	0
		AAA, AAG mix	3 (4.1)	2 (2.7)
	Arg	AGA	3 (4.1)	0
	No reaction		-	31 (41.9)
70	Lys	AAA	62 (83.8)	61 (82.4)
		AAG	2 (2.7)	0
	Arg	AGA	8 (10.8)	8 (10.8)
		AGG	1 (1.4)	1 (1.4)
	Lys, Arg mix		1 (1.4)	0
	No reaction		-	4 (5.4)
103	Lys	AAA	60 (82.2)	50 (68.5)
		AAG	1 (1.4)	0
		AAA, AAG mix	1 (1.4)	0
	Asn	AAC	4 (5.5)	2 (2.7)
		AAT	2 (2.7)	2 (2.7)
		AAC, AAT mix	1 (1.4)	1 (1.4)
	Arg	AGA	4 (5.5)	0
	No reaction		-	18 (24.7)
184	Met	ATG	52 (71.2)	46 (63.0)
	Val	GTG	19 (26.0)	16 (21.9)
		GTA	1 (1.4)	0
	Met, Val mix		1 (1.4)	1 (1.4)
	No reaction		-	10 (13.7)
215	Thr	ACC	48 (65.8)	46 (63.0)
	Tyr	TAC	16 (21.9)	15 (20.5)
	Phe	TTC	6 (8.2)	6 (8.2)
	Thr, Tyr mix		1 (1.4)	1 (1.4)
	Other		2 (2.7)	0
	No reaction		-	5 (6.8)

doi:10.1371/journal.pone.0109823.t002

Identification of DR mutations in clinical specimens by the PCR-SSOP-Luminex DR assay

We performed the PCR-SSOP-Luminex DR assay on 74 specimens whose DR mutations had been sequenced (Fig. 4). The lowest MFI of five standard probes (MFI = 837.5) was assumed as the cut off value for the positive signal. We synthesized two additional wild-type oligoprobes (K70K-AAA-2 and T215T-ACC-2), since the original oligobeads (K70K-AAA-1 and T215T-ACC-1) gave marginal signals in some specimens (Table 1 and Fig. 4). By the modification of the position of the target codons and the length of flanking sequences, we could obtain higher MFI signals. Successful determination of the genotypes was 62/74 (83.8%), 43/74 (58.1%), 70/74 (94.6%), 55/73 (75.3%), 63/73 (86.3%) and 68/73 (93.2%) for M41, K65, K70, K103, M184 and T215, respectively. The median of background signal (without sample) was MFI = 178, and median negative signal from the patients sample was MFI = 181 (interquartile range (IQR) = 101–307). PCR-SSOP-Luminex assays create very low background and non-specific signal from negative samples. When the genotype was successfully determined by the PCR-SSOP-Luminex assay, the results were always concordant with those of sequencing (Table 2). We inferred that the failure to determine the genotype was due to sequence diversities. Therefore, we decided to customize the assay according to the sequences around K65 which had the lowest success rate (58.1%).

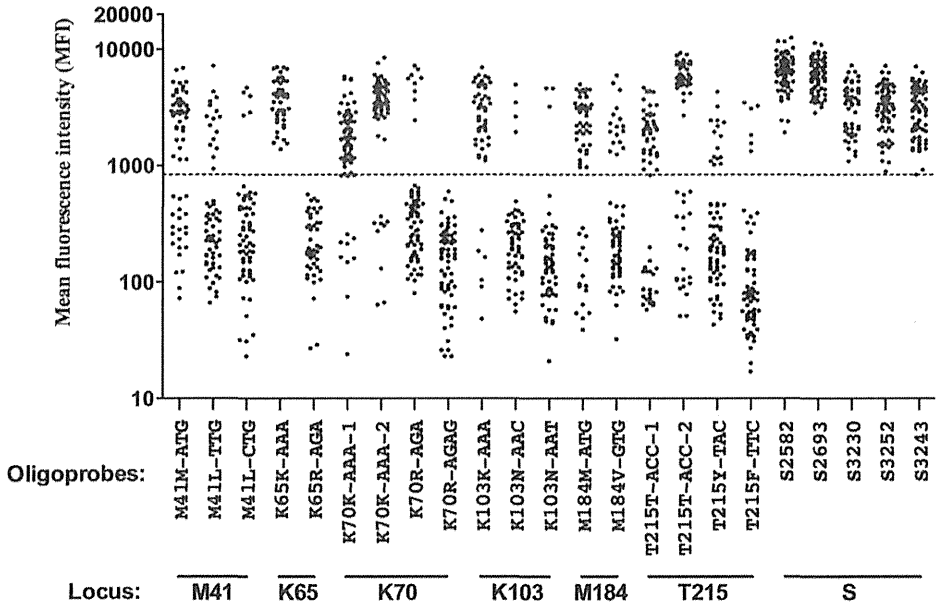

Figure 4. PCR-SSOP-Luminex DR assay of clinical samples. Results of 18 probes for 6 DR loci and 5 standard probes are shown. Each dot represents the mean of triplicates. Dashed line indicates the cut-off value, the lowest MFI among 5 standard probes (MFI = 837.5).
doi:10.1371/journal.pone.0109823.g004

Customization of oligoprobes to detect genetic diversity around K65

In 31 specimens without signals, the sequence around K65 was very diverse, especially at codons K65, K66 and K67 (Table 3). The nucleotide position of A2723G, A2747G and C2750T were frequent polymorphism for the wild type amino acid K65, K66 and D67, respectively. Fourteen specimens had a G2748A mutation that led to D67N, a thymidine analogue mutation [19]. Based on these results we synthesized 10 additional oligoprobes (Table 4).

The specificity of the newly added oligoprobes was confirmed by the plasmids carrying the mutation (data not shown). Customization of the assay decreased the number of specimens without signals from 31 to 6 (Fig. 5).

Discussion

We developed a PCR-SSOP-Luminex DR assay that can identify 6 clinically important DR mutations for NRTI and NNRTI in a single well. To simplify the development, we chose clade B virus and focused on the following mutations in the RT region: M41L, K65R, K70R, K103N, M184V and T215Y/F. We designed a series of capture probes according to the database of the Japanese patients. MFI from hybridization with the corresponding probes was greater than 20-fold signal-to-noise ratio in plasmid experiments (Fig. 2), at least 2-fold signal-to-noise ratio using clinical samples (Fig. 4). The initial positive reaction was as low as 58.1% (43/74) in the highly polymorphic K65 region. The use of additional probes designed to match sequences in the patients' specimens improved the detection rate to 91.9% (68/74), demonstrating that the PCR-SSOP-Luminex assay can be customized to reflect sequences of the viruses prevalent in a given environment.

Transmission of viral strains with major DR mutations can reduce the efficacy of first-line regimens. Since the first report of a horizontal transmission of HIV-1 harboring a zidovudine-resistant mutation [20], 5% to 15% of treatment-naïve, HIV-1-infected individuals harbored the viruses with DR mutations in early 2000s in resource-rich settings [21–24]. It was suggested that transmission of drug resistance in the resource-rich settings can remain stable and at a low level [25]. However, in Japan where the transmission of drug-resistant viruses has historically been low, there seems to be an increasing trend [18,26]. Rates of transmitted HIV drug resistance has remained limited also in resource-limited settings (http://www.who.int/hiv/topics/drugresistance/en/), however, limitation on the first line and subsequent regimens would be a concern. Continued surveillance of drug resistant HIV-1 is warranted.

There are some multiplex strategies to detect the single-nucleotide differences, LigAmp assay [27,28], Nanostring assays [29], oligonucleotide ligation assay-based DNA chip [30], AS-PCR [31,32]. These assays provide substantial improvements in their detection sensitivity over conventional sequencing-based assays, however major limitation of these assays could be detecting one or few DR mutations at a time. PCR-SSOP-Liminex assay should be able to accommodate more DR mutations than the others.

One limitation of PCR-SSOP-Luminex assay is the assay sensitivity caused by diversity of HIV. We were able to detect DR mutations that constituted 10% of the mixture in the isogenic system using plasmids. Even after successful amplification, we could not get signal in considerable number of patient's specimens. By comparison with cloning and sequencing, we estimate that at least 20% mutant was necessary in the patient's specimens to be detected by the PCR-SSOP-Luminex assay. The sensitivity of detection by Sanger sequencing has been reported to be ~20% [33,34]. Sanger sequencing and PCR-SSOP-Luminex had approximately the same detection sensitivity on patient materials. In Sanger sequencing, nucleotide sequences are determined by the wave height. When the virus in the plasma is a mixture of the wild type and a mutant, each nucleotide is displayed as two waves in the same locus with different height according to the fraction in the sample. In the case of PCR-SSOP-Luminex, the wild type or mutant nucleotides are detected independently by the signal bound to the proper probes. Therefore, as we showed partly in this paper, the mutant detection by PCR-SSOP-Luminex assay could

Table 3. Sequence diversity around K65 in the 31 specimens.

Amino acid (HXB2-wt)	I63 K64 K65 K66 D67 S68	
Nucleotide (HXB2-wt)	**ATA AAG AAA AAA GAC AGT**	**Number of specimens**
	2747	
K66K-AAG	— — — —G — —	10
	2747 2748	
K66K-AAG/D67N-AAC	— — — —G A— —	5
	2748	
D67N-AAC	— — — — A— —	3
	2750	
D67D-GAT	— — — — —T —	1
	2748	
K65K-AAG/D67N-AAC	— — —G — A— —	2
	2748	
K65K-AAR/D67N-AAC	— — —R — A— —[a]	1
	2747 2748	
K65K-AAG/K66K-AAG/D67N-AAC	— — —G —G A— —	1
	2741 2748	
K65K-AAG/D67N-AAC/K64K-AAA	— —A —G — A— —	1
	2747 2750	
K66K-AAG/D67D-GAT	— — — —G —T —	1
	2748 2750	
D67N-AAT	— — — — A-T —	1
	2750 2751	
D67D-GAT/S68G-GGT	— — — — —T G-	2
	2747	
K65R-AGA/K66K-AAG	— — -G- —G — —	1
	2750	
K65R-AGA/D67D-GAT	— — -G- — —T —	2

[a]R: Mixed base of A and G.

doi:10.1371/journal.pone.0109823.t003

be improved by further customization to the circulating viruses. In our paper, we used maximum 23 oligoprobes in one tube or well. The evaluation of assay volume etc. would be necessary to determine actually possible maximum number of ologibrobes in

Table 4. Design of additional oligoprobes based on clinical samples.

Locus	Name of probe	Oligoprobes	Nucleotide sequence (5′-3′)
K65			ATA AAG AAA AAA GAC AGT ACT
	K66K-AAG	ATAAAGAAAAAGGACAG	— — — —G — —
	K65R-AGA/K66K-AAG	ATAAAGAGAAAGGACAG	— — -G- —G — —
	K66K-AAG/D67N-AAC	ATAAAGAAAAAGAACAG	— — — —G A— —
	K65R-AGA/K66K-AAG/D67N-AAC	ATAAAGAGAAAGAACAG	— — -G- —G A— —
	D67N-AAC	ATAAAGAAAAAAAACAGT	— — — — A— —
	K65R-AGA/D67N-AAC	ATAAAGAGAAAAAACAG	— — -G- — A— —
	D67D-GAT	ATAAAGAAAAAAGATAGT	— — — — —T —
	K65R-AGA/D67D-GAT	ATAAAGAGAAAAGATAGT	— — -G- — —T —
	K65K-AAG	ATAAAGAAGAAAGACAG	— — —G — — —
	K65K-AAG/D67N-AAC	ATAAAGAAGAAAAACAGTA	— — —G — A— — -

doi:10.1371/journal.pone.0109823.t004

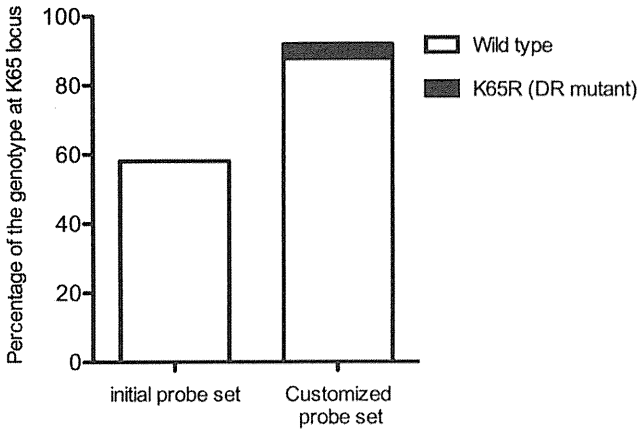

Figure 5. Improvement of the detection by the additional probes at K65 locus. The ordinate shows the percentage of the genotype at K65 locus determined by the PCR-SSOP-Luminex DR assay. One hundred % is the sample number (74) successfully amplified by PCR.
doi:10.1371/journal.pone.0109823.g005

one tube. 100 color-coded beads are available, theoretically, 100 probes could be applied (http://www.luminexcorp.com/Products/Instruments/Luminex100200/). Since the wild type or mutant nucleotides are detected as the signal of hybridized probes for each in the PCR-SSOP-Luminex assay, inclusion of multiplex probes based on the codon usages for the DR mutations and the sequence variations in the flanking region of circulating viruses would improve the detection. According to our results, we could develop, validate and customized PCR-SSOP-Luminex assay for detecting DR mutations at six positions in HIV-1 RT gene. The study numbers are very limited and we worked only on subtype B HIV-1 in this article. HIV-1 diversity is notoriously huge and sequences in an individual could be more diverse than acutely expanding viruses in the field [35]. Diagnostic use in individual patients is far from the actual application at present. We believe the assay would be more suitable for molecular epidemiological studies detecting regional trends of HIV-1 DR mutation over time.

PCR-SSOP-Luminex assay were widely used for the detection of papillomavirus, influenza surveillance etc. in developing countries [36,37]. Furthermore, application of Luminex technology to other pathogen (*C. difficile*, *Norovirus*, *E. coli* or *Salmonella*, *Rotavirus A*, *Campylobacter*, *Shigella* etc.) were reported recently [38]. It would be feasible to expect that the use of Luminex technology will be wide-spread in the near future. Furthermore, the application of PCR-SSOP-Luminex DR assay to non-clade B HIV-1 is currently under development. Future studies include refinement of the assay for use with specimens co-infected with HIV-1 and HBV.

Conclusions

We have developed a rapid high-throughput assay for DR testing. The assay can be customized by adding oligoprobes suitable for the circulating viruses. The assay may turn out to be a useful method especially for public health research in both resource-rich and resource-limited settings.

Acknowledgments

The authors thank Dr. Barbara Rutledge for discussion and editing English.

Author Contributions

Conceived and designed the experiments: LG NH AKT AI. Performed the experiments: LG NH AKT. Analyzed the data: LG NH TS WS. Contributed reagents/materials/analysis tools: MM. Contributed to the writing of the manuscript: LG NH AI. Provided clinical information and patient care: HN MK TK EA TK AI. Discussion: TI GFG.

References

1. Palella FJ Jr, Delaney KM, Moorman AC, Loveless MO, Fuhrer J, et al. (1998) Declining morbidity and mortality among patients with advanced human immunodeficiency virus infection. HIV Outpatient Study Investigators. N Engl J Med 338: 853–860.
2. Samji H, Cescon A, Hogg RS, Modur SP, Althoff KN, et al. (2013) Closing the Gap: Increases in Life Expectancy among Treated HIV-Positive Individuals in the United States and Canada. PLoS One 8: e81355.
3. Frentz D, Boucher CA, van de Vijver DA (2012) Temporal changes in the epidemiology of transmission of drug-resistant HIV-1 across the world. AIDS Rev 14: 17–27.
4. WHO (2012) WHO HIV Drug Resistance Report 2012. WHO Press.
5. WHO (2013) Consolidated guidelines on the use of antiretroviral drugs for treating and preventing HIV infection: Recommendations for a public health approach. WHO Press.
6. Sungkanuparph S, Techasathit W, Utaipiboon C, Chasombat S, Bhakeecheep S, et al. (2010) Thai national guidelines for antiretroviral therapy in HIV-1 infected adults and adolescents 2010. Asian Biomedicine 4: 515–528.
7. Clavel F, Hance AJ (2004) HIV drug resistance. N Engl J Med 350: 1023–1035.
8. Wainberg MA, Friedland G (1998) Public health implications of antiretroviral therapy and HIV drug resistance. Jama 279: 1977–1983.
9. Shafer RW, Rhee SY, Pillay D, Miller V, Sandstrom P, et al. (2007) HIV-1 protease and reverse transcriptase mutations for drug resistance surveillance. Aids 21: 215–223.
10. Balajee SA, Sigler L, Brandt ME (2007) DNA and the classical way: identification of medically important molds in the 21st century. Med Mycol 45: 475–490.
11. Dunbar SA (2006) Applications of Luminex xMAP technology for rapid, high-throughput multiplexed nucleic acid detection. Clin Chim Acta 363: 71–82.
12. Itoh Y, Mizuki N, Shimada T, Azuma F, Itakura M, et al. (2005) High-throughput DNA typing of HLA-A, -B, -C, and -DRB1 loci by a PCR-SSOP-Luminex method in the Japanese population. Immunogenetics 57: 717–729.
13. Wensing AM, Calvez V, Gunthard HF, Johnson VA, Paredes R, et al. (2014) 2014 update of the drug resistance mutations in HIV-1. Top Antivir Med 22: 642–650.
14. Cheng-Mayer C, Quiroga M, Tung JW, Dina D, Levy JA (1990) Viral determinants of human immunodeficiency virus type 1 T-cell or macrophage tropism, cytopathogenicity, and CD4 antigen modulation. J Virol 64: 4390–4398.
15. Shioda T, Levy JA, Cheng-Mayer C (1991) Macrophage and T cell-line tropisms of HIV-1 are determined by specific regions of the envelope gp120 gene. Nature 349: 167–169.
16. Ho SN, Hunt HD, Horton RM, Pullen JK, Pease LR (1989) Site-directed mutagenesis by overlap extension using the polymerase chain reaction. Gene 77: 51–59.
17. Koga I, Odawara T, Matsuda M, Sugiura W, Goto M, et al. (2006) Analysis of HIV-1 sequences before and after co-infecting syphilis. Microbes Infect 8: 2872–2879.
18. Hattori J, Shiino T, Gatanaga H, Yoshida S, Watanabe D, et al. (2010) Trends in transmitted drug-resistant HIV-1 and demographic characteristics of newly diagnosed patients: nationwide surveillance from 2003 to 2008 in Japan. Antiviral Res 88: 72–79.
19. Johnson VA, Calvez V, Gunthard HF, Paredes R, Pillay D, et al. (2013) Update of the drug resistance mutations in HIV-1: March 2013. Top Antivir Med 21: 6–14.
20. Erice A, Mayers DL, Strike DG, Sannerud KJ, McCutchan FE, et al. (1993) Brief report: primary infection with zidovudine-resistant human immunodeficiency virus type 1. N Engl J Med 328: 1163–1165.
21. Cane P, Chrystie I, Dunn D, Evans B, Geretti AM, et al. (2005) Time trends in primary resistance to HIV drugs in the United Kingdom: multicentre observational study. Bmj 331: 1368.
22. Descamps D, Chaix ML, Andre P, Brodard V, Cottalorda J, et al. (2005) French national sentinel survey of antiretroviral drug resistance in patients with HIV-1 primary infection and in antiretroviral-naive chronically infected patients in 2001–2002. J Acquir Immune Defic Syndr 38: 545–552.

23. Weinstock HS, Zaidi I, Heneine W, Bennett D, Garcia-Lerma JG, et al. (2004) The epidemiology of antiretroviral drug resistance among drug-naive HIV-1-infected persons in 10 US cities. J Infect Dis 189: 2174–2180.
24. Wensing AM, van de Vijver DA, Angarano G, Asjo B, Balotta C, et al. (2005) Prevalence of drug-resistant HIV-1 variants in untreated individuals in Europe: implications for clinical management. J Infect Dis 192: 958–966.
25. Yerly S, von Wyl V, Ledergerber B, Boni J, Schupbach J, et al. (2007) Transmission of HIV-1 drug resistance in Switzerland: a 10-year molecular epidemiology survey. Aids 21: 2223–2229.
26. Gatanaga H, Ibe S, Matsuda M, Yoshida S, Asagi T, et al. (2007) Drug-resistant HIV-1 prevalence in patients newly diagnosed with HIV/AIDS in Japan. Antiviral Res 75: 75–82.
27. Shi C, Eshleman SH, Jones D, Fukushima N, Hua L, et al. (2004) LigAmp for sensitive detection of single-nucleotide differences. Nat Methods 1: 141–147.
28. Church JD, Towler WI, Hoover DR, Hudelson SE, Kumwenda N, et al. (2008) Comparison of LigAmp and an ASPCR assay for detection and quantification of K103N-containing HIV variants. AIDS Res Hum Retroviruses 24: 595–605.
29. Geiss GK, Bumgarner RE, Birditt B, Dahl T, Dowidar N, et al. (2008) Direct multiplexed measurement of gene expression with color-coded probe pairs. Nat Biotechnol 26: 317–325.
30. Deng JY, Zhang XE, Mang Y, Zhang ZP, Zhou YF, et al. (2004) Oligonucleotide ligation assay-based DNA chip for multiplex detection of single nucleotide polymorphism. Biosens Bioelectron 19: 1277–1283.
31. Boltz VF, Ambrose Z, Kearney MF, Shao W, Kewalramani VN, et al. (2012) Ultrasensitive allele-specific PCR reveals rare preexisting drug-resistant variants and a large replicating virus population in macaques infected with a simian immunodeficiency virus containing human immunodeficiency virus reverse transcriptase. J Virol 86: 12525–12530.
32. Rowley CF, Boutwell CL, Lockman S, Essex M (2008) Improvement in allele-specific PCR assay with the use of polymorphism-specific primers for the analysis of minor variant drug resistance in HIV-1 subtype C. J Virol Methods 149: 69–75.
33. Zagordi O, Klein R, Daumer M, Beerenwinkel N (2010) Error correction of next-generation sequencing data and reliable estimation of HIV quasispecies. Nucleic Acids Res 38: 7400–7409.
34. Mohamed S, Ravet S, Camus C, Khiri H, Olive D, et al. (2014) Clinical and analytical relevance of NNRTIs minority mutations on viral failure in HIV-1 infected patients. J Med Virol 86: 394–403.
35. Walker BD, Korber BT (2001) Immune control of HIV: the obstacles of HLA and viral diversity. Nat Immunol 2: 473–475.
36. Jiang HL, Zhu HH, Zhou LF, Chen F, Chen Z (2006) Genotyping of human papillomavirus in cervical lesions by L1 consensus PCR and the Luminex xMAP system. J Med Microbiol 55: 715–720.
37. Vongphrachanh P, Simmerman JM, Phonekeo D, Pansayavong V, Sisouk T, et al. (2010) An early report from newly established laboratory-based influenza surveillance in Lao PDR. Influenza Other Respir Viruses 4: 47–52.
38. Claas EC, Burnham CA, Mazzulli T, Templeton K, Topin F (2013) Performance of the xTAG(R) gastrointestinal pathogen panel, a multiplex molecular assay for simultaneous detection of bacterial, viral, and parasitic causes of infectious gastroenteritis. J Microbiol Biotechnol 23: 1041–1045.

World Journal of Gastroenterology

Online Submissions: http://www.wjgnet.com/esps/
bpgoffice@wjgnet.com
doi:10.3748/wjg.v20.i15.4316

World J Gastroenterol 2014 April 21; 20(15): 4316-4328
ISSN 1007-9327 (print) ISSN 2219-2840 (online)

ORIGINAL ARTICLE

Non-transmissible Sendai virus vector encoding *c-myc* suppressor FBP-interacting repressor for cancer therapy

Kazuyuki Matsushita, Hideaki Shimada, Yasuji Ueda, Makoto Inoue, Mamoru Hasegawa, Takeshi Tomonaga, Hisahiro Matsubara, Fumio Nomura

Kazuyuki Matsushita, Fumio Nomura, Department of Molecular Diagnosis, Graduate School of Medicine, Chiba University, Chiba 260-8670, Japan
Hideaki Shimada, Department of Surgery, School of Medicine, Toho University, Tokyo 143-8541, Japan
Yasuji Ueda, Makoto Inoue, Mamoru Hasegawa, DNAVEC Corporation, 6 Ohkubo, Tsukuba City, Ibaraki 300-2611, Japan
Takeshi Tomonaga, Proteome Research Center, Proteome Research Project, National Institute of Biomedical Innovation, Osaka 567-0085, Japan
Hisahiro Matsubara, Department of Frontier Surgery, Chiba University, Graduate School of Medicine, Chiba 260-8670, Japan
Author contributions: Matsushita K designed the research; Matsushita K, Ueda Y and Inoue M performed the research; Shimada H, Tomonaga T, Hasegawa M, Matsubara H and Nomura F contributed new reagents/analytic tools and scientific discussions; Matsushita K analyzed the data and wrote the paper.
Supported by In part by the 21st Century COE (Center Of Excellence) Programs to Dr. Takenori Ochiai and by a Grant-in-Aid 18591453 to K.M from the Ministry of Education, Science, Sports and Culture of Japan
Correspondence to: Kazuyuki Matsushita, MD, PhD, Associate Professor, Department of Molecular Diagnosis, Graduate School of Medicine, Chiba University, 1-8-1 Inohana, Chuo-Ku, Chiba 260-8670, Japan. kmatsu@faculty.chiba-u.jp
Telephone: +81-43-2227171 Fax: +81-43-2262169
Received: October 22, 2013 Revised: December 14, 2013
Accepted: January 19, 2014
Published online: April 21, 2014

Abstract

AIM: To investigate a novel therapeutic strategy to target and suppress *c-myc* in human cancers using far up stream element (FUSE)-binding protein-interacting repressor (FIR).

METHODS: Endogenous c-Myc suppression and apoptosis induction by a transient FIR-expressing vector was examined *in vivo via* a HA-tagged FIR (HA-FIR) expression vector. A fusion gene-deficient, non-transmissible, Sendai virus (SeV) vector encoding FIR cDNA, SeV/dF/FIR, was prepared. SeV/dF/FIR was examined for its gene transduction efficiency, viral dose dependency of antitumor effect and apoptosis induction in HeLa (cervical squamous cell carcinoma) cells and SW480 (colon adenocarcinoma) cells. Antitumor efficacy in a mouse xenograft model was also examined. The molecular mechanism of the anti-tumor effect and c-Myc suppression by SeV/dF/FIR was examined using Spliceostatin A (SSA), a SAP155 inhibitor, or SAP155 siRNA which induce c-Myc by increasing FIRΔexon2 in HeLa cells.

RESULTS: FIR was found to repress *c-myc* transcription and in turn the overexpression of FIR drove apoptosis through *c-myc* suppression. Thus, FIR expressing vectors are potentially applicable for cancer therapy. FIR is alternatively spliced by SAP155 in cancer cells lacking the transcriptional repression domain within exon 2 (FIRΔexon2), counteracting FIR for c-Myc protein expression. Furthermore, FIR forms a complex with SAP155 and inhibits mutual well-established functions. Thus, both the valuable effects and side effects of exogenous FIR stimuli should be tested for future clinical application. SeV/dF/FIR, a cytoplasmic RNA virus, was successfully prepared and showed highly efficient gene transduction in *in vivo* experiments. Furthermore, in nude mouse tumor xenograft models, SeV/dF/FIR displayed high antitumor efficiency against human cancer cells. SeV/dF/FIR suppressed SSA-activated c-Myc. SAP155 siRNA, potentially produces FIR Δexon2, and led to c-Myc overexpression with phosphorylation at Ser62. HA-FIR suppressed endogenous c-Myc expression and induced apoptosis in HeLa and SW480 cells. A *c-myc* transcriptional suppressor FIR expressing SeV/dF/FIR showed high gene transduction efficiency with significant antitumor effects and apoptosis induction in HeLa and SW480 cells.

CONCLUSION: SeV/dF/FIR showed strong tumor growth

suppression with no significant side effects in an animal xenograft model, thus SeV/dF/FIR is potentially applicable for future clinical cancer treatment.

Key words: Cancer gene therapy; *c-myc* suppressor; Far up stream element-binding protein-interacting repressor; Sendai virus vector

Core tip: The authors performed *in vivo* experiments and included an animal model to examine the Sendai virus/dF/Far Up Stream Element-Binding Protein-Interacting Repressor for cancer gene therapy to minimize side effects for clinical use.

Matsushita K, Shimada H, Ueda Y, Inoue M, Hasegawa M, Tomonaga T, Matsubara H, Nomura F. Non-transmissible Sendai virus vector encoding *c-myc* suppressor FBP-interacting repressor for cancer therapy. *World J Gastroenterol* 2014; 20(15): 4316-4328 Available from: URL: http://www.wjgnet.com/1007-9327/full/v20/i15/4316.htm DOI: http://dx.doi.org/10.3748/wjg.v20.i15.4316

INTRODUCTION

c-Myc plays an essential role in cell proliferation and tumorigenesis. *c-myc* activation was also shown to be required for skin epidermal and pancreatic beta-cell tumor maintenance in c-MYC-ER^{TAM} transgenic mice[1]. High *c-myc* expression level in colorectal cancer tissues was associated with poor long-term survival of colorectal cancer patients[2]. The far up stream element (FUSE) is a sequence required for correct expression of the human *c-myc* gene[3]. The FUSE is located at 1.5 kb upstream of *c-myc* promoter P1, and binds the FUSE binding protein (FBP), a transcription factor which stimulates *c-myc* expression in a FUSE-dependent manner[4]. Yeast two-hybrid analysis revealed that FBP binds to a protein that has transcriptional inhibitory activity termed the FBP interacting repressor (FIR). FIR interacts with the central DNA binding domain of FBP[5]. Recently, FIR was found to engage the TFIIH/p89/XPB helicase and repress *c-myc* transcription by delaying promoter escape[5,6]. Furthermore, exogenous FIR expression represses endogenous *c-myc* transcription, and drives apoptosis due to the decrease in c-Myc[7]. Although these observations indicate that cancer therapies targeting *c-myc* suppression by FIR may be a useful strategy, the mechanism of the antitumor effect of FIR should be determined in detail prior to clinical testing. For example, first, FIR is alternatively spliced in colorectal cancer lacking the transcriptional repression domain within exon 2 (FIRΔexon2)[7]. Second, FIR and FIRΔexon2 form a homo- or hetero-dimer, which complexes with SAP155, a subunit of the essential splicing factor 3b (SF3b) subcomplex in the spliceosome, and is required for correct P27Kip1 (P27) pre-mRNA splicing, after which P27 arrests cells in G1[8]. Third, SAP155 is required for correct FIR pre-mRNA splicing and thus the FIR/FIRΔexon2/SAP155 interaction bridged *c-myc* and p27 expression[9]. Accordingly, SAP155-mediated alternative splicing of FIR serves as a molecular switch for *c-myc* expression[9]. Finally, spliceostatin A (SSA), a natural SF3b inhibitor, markedly inhibited P27 expression by disrupting its pre-mRNA splicing and reducing cdk2/cyclinE expression[10]. Taken together, these findings suggest that exogenous FIR stimuli potentially affect the FIR/FIRΔexon2/SAP155 interaction which is pivotal for the cell cycle, cancer development and differentiation.

In this study, a fusion gene-deficient human FIR-expressing Sendai virus vector (SeV/dF/FIR) was prepared for future cancer therapy for the following reasons; Sendai virus (SeV), a member of the Paramyxoviridae family, has envelopes and a nonsegmented negative-strand RNA genome. The SeV genome contains six major genes in tandem on a single negative-strand RNA. Three proteins, the nucleoprotein (NP), phosphoprotein (P) and large protein (L; the catalytic subunit of the polymerase) form a ribonucleoprotein complex (RNP) with the SeV RNA. Matrix proteins (M) contribute to the assembly of viral particles, hemagglutinin-neuraminidase (HN) and fusion proteins (F) engage in the attachment of viral particles and infiltration of RNPs into infected cells. Importantly, SeV does not transform cells by integrating its genome into the cellular genome[11]. Therefore, SeV can mediate gene transfer and expression to a cytoplasmic location using cellular tubulin[12], thereby avoiding possible malignant transformation due to the genetic alteration of host cells. These are the safety advantages of SeV. Recently, a novel SeV vector was established where an enhanced green fluorescent protein (EGFP) reporter gene was inserted at the 3'-end of fusion gene-deficient SeV genomic RNA (SeV/dF/EGFP)[13]. This SeV/dF/EGFP is incapable of self-replication, but capable of infecting various cells, including human smooth muscle cells, hepatocytes, and endothelial cells, thus the SeV/dF/EGFP has a broad spectrum of gene transfer activity[9,10]. In this study, SeV/dF/FIR was prepared following the method for SeV/dF/EGFP[12,13]. The validity of SeV/dF/FIR for cancer therapy was examined in animal xenograft models as SeV/dF vectors have been shown to be applicable for clinical use[14-18]. The clinical use of SeV/dF/FIR for cancer therapy is also discussed.

MATERIALS AND METHODS

Plasmids

Full-length FIR cDNA (HA-FIR) was cloned into the pCGNM2 vector plasmid to introduce the hemagglutinin (HA)-tag at the amino termini[7]. Full-length FIR cDNA was cloned into the p3xFLAG-CMV-14 vector (Sigma, MO, United States) to introduce the Flag-tag at the amino termini for the selection of FIR-Flag in 293T cells (performed by Dr. T.N.). Plasmids were prepared by

CsCl ultra-centrifugation or the Endofree® Plasmid Maxi Kit (Qiagen, MD, United States) and the DNA sequences were verified.

Tumor cell lines

HeLa cells (human cervical squamous cell carcinoma cells), LoVo and SW480 cells (human colon cancer cell lines) and LLC-MK2 a rhesus monkey kidney cell line were purchased from the American Type Culture Collection (Manassas, VA, United States). Yes-5, a human esophageal squamous cell carcinoma cell line was established by Dr Takuo Murakami (Yamaguchi University, Yamaguchi, Japan). All cell lines were cultured at 37 ℃ in a humidified atmosphere containing 5% CO_2. All tumor cell lines, except LLC-MK2 cells [which were maintained in DMEM; Dulbecco's Modified Eagle's Medium (Gibco BRL, NY, United States)] were cultured in tissue flasks or Petri dishes containing RPMI-1640 (Gibco, NY, United States) supplemented with 10% heat-inactivated FBS and penicillin (100 units/mL), streptomycin (0.1 mg/mL), and 2 mmol/L glutamine.

Immunocytochemistry, protein extraction and immunoblotting

Immunocytochemistry was performed as described previously[7]. Protein extraction and immunoblotting are described elsewhere[8,9].

siRNA against FIR or SAP155

SAP155 siRNA duplexes were purchased from Sigma Aldrich. The target sequences for SAP155 siRNA oligonucleotides were listed previously[8]. Luciferase GL2 duplex was used as a negative control for siRNA targeting 5'-CGTACGCGGAATACTTCGA-3'. Transient transfection of siRNA was carried out using Lipofectamine 2000 (Invitrogen) according to the manufacturer's instructions. The transfected cells were cultured for 72 h at 37 ℃ in a 5% CO_2 incubator.

Apoptosis detection

Apoptotic cells were detected by terminal deoxynucleotidyl transferase dUTP nick end labeling (TUNEL) assay according to the manufacturer's instructions (Apoptosis Detection System, Fluorescein, Promega, WI, United States) as described previously[7]. Apoptosis detection by APOPercentage apoptosis assay™ (Funakoshi Co., Ltd., Tokyo, Japan) was performed according to the manufacturer's instructions[9].

Construction of SeV vector

Human FIR cDNA was amplified with a pair of NotI site-tagged primers containing SeV-specific transcriptional regulatory signal sequences, (End and Start, italicized below) 5'-ATTGCGGCCGCCAAGGTTCAATGGCGACGGCGACCATAGC-3' and 5'-ATTGCGGCCGCGATGAACTTTCACCCTAAGTTTTTCTTACTACGGTCACGCAGAGAGGTCACTGTTATCAAAACGC-3'. The amplified fragment was introduced into the NotI site of the parental SeV vector cDNA, $pSeV^{18+}b(+)/dF$[15], to generate $pSeV^{18+}$hFIR/dF. $pSeV^{18+}$hFIR/dF was transfected to LLC-MK2 cells which were preliminarily infected with psoralen- and long-wave UV-treated vaccinia virus vTF7-3, expressing T7 polymerase. The cells were then washed twice with DMEM, and cultured for 24 h in DMEM containing cytosine β-D-arabinofuranoside (AraC; 40 μg/mL) and trypsin (7.5 μg/mL). LLC-MK2/F7/A cells expressing the F protein were suspended in DMEM containing AraC and trypsin, and layered onto the transfected cells, and cultured at 37 ℃ for an additional 48 h. The recovered vector in the culture supernatants was propagated using the LLC-MK2/F7/A cells. A GFP expression vector (SeV/dF/GFP) was prepared as previously described[8]. The viral vectors were further amplified by several rounds of propagation. The virus titers of the recovered vectors were determined by their infectivity and expressed using cell-infectious units (CIU). These vectors were frozen at -80 ℃ until use.

SeV/dF/GFP-mediated green fluorescent protein transduction efficiency

One million LLC-MK2 cells and HeLa cells were seeded in six-well plates and transduced with SeV/dF/GFP when monolayers reached 60%-80% confluence. As the standard inoculation procedure for vaccination, the monolayers were washed twice with PBS and overlaid with serum-free medium containing SeV/dF/GFP at a multiplicity of infection (MOI) of 0, 1, 10, 50, 100, or 300. After incubation at 37 ℃ for 90 min, non-adsorbed virus was removed, medium containing 10% FBS was added, and the cells were incubated for more than 48 h at 37 ℃. The transduction studies were carried out in triplicate for each MOI. Microscopy was used to detect transduced cells by GFP fluorescence. At 72 h after transduction, the GFP-transduced cells were analyzed for GFP expression using a FACS Calibrator (BD Pharmingen, Franklin Lakes, NJ, United States).

MTS assay to assess cell viability

The inhibitory effects of viruses on the proliferation of cultured cells were examined using the CellTiter96™ AQ_{ueous} One Solution Proliferation Assay (Promega, Madison, WI, United States). In brief, five thousand cells were plated in each well on day 0. On day 1, 24 h later, HeLa cells were infected with SeV/dF/FIR or SeV/dF/GFP as the control at 0.1 to 10 MOI, and cultured for 2 d. On day 3, cell viability was quantified by measuring the absorbance at 570 nm after incubation with the tetrazolium compound [3-(4,5-dimethylthiozol-2-yl)-5-(3-carboxymethoxyphenyl)-2-(4-sulfophenyl)-2H-tetrazolium, inner salt (MTS), and an electron coupling agent, phenazine ethosulfate (PES)] (Promega, Madison, WI, United States) for 4 h. The absorbance at 570 nm was measured by a Mutiabel Counter™, ARVOSX WAIIAC™ (Perkin Elmer, MA, United States). The results are shown as percentages of the uninfected control cells.

Mice

Six- to eight-week male immuno-competent Balbc/nu/

nu mice were purchased from Clea Japan (Tokyo, Japan) and housed in the Animal Maintenance Facility at Chiba University under specific pathogen-free conditions. All animal experiments were approved by the Committee of the Ethics on Animal Experiments in the Faculty of Medicine, Chiba University and carried out following the Guidelines for Animal Experiments in the Faculty of Medicine, Chiba University, Chiba, Japan and The Law and Notification of the Government. Mouse experiments were carried out at least twice to confirm the results.

Tumor xenograft experiments

The *in vivo* inhibition of tumorigenicity of HeLa cells (human cervical squamous cell carcinoma cells) was examined by SeV/dF/FIR or SeV/dF/GFP injection (as the control). 5×10^6 cells/50 μL PBS of HeLa cells were injected under the skin in the right thigh of nude mice (6-wk old males). Tumor growth was observed and the long and short diameter measured for tumor volume calculation. Thirty days after inoculation, tumors grew up to 5-8 mm in diameter in 18 of 18 mice (100%). Tumor size was calculated using the formula, $(a \times b^2)/2$, where a and b represent the larger and smaller diameters, respectively, and was monitored every 3 d.

FIR-binding protein identification

The methods for the direct nanoflow liquid chromatography-tandem mass spectrometry system with FIR-FLAG transiently transfected 293T nuclear extracts have been described previously[19-23].

RESULTS

HA-FIR suppresses endogenous c-Myc expression with apoptosis induction in vivo

To examine endogenous *c-myc* gene suppression by FIR, HA-FIR expression plasmids were transfected into HeLa cells, and c-Myc expression was visualized by immunostaining with anti-c-Myc antibodies (Figure 1A; upper panels: HA-FIR is red; c-Myc is green). c-Myc levels were greatly diminished in HA-FIR expressing cells (arrows), demonstrating that FIR represses endogenous c-Myc expression in SW480 (Figure 1A; middle panels) and LoVo cells (Figure 1A; lower panels). After HA-FIR expression plasmids were transfected into HeLa, SW480 or LoVo cells, apoptotic cells were visualized by TUNEL assay. HA-FIR transfected cells were definitively associated with apoptosis (Figure 1B).

FIR protein expression by fusion gene-deficient SeV/dF/FIR

SeV/dF/FIR and SeV/dF/GFP were prepared as described in Materials and Methods (Figure 2A, B). SeV/dF/FIR vectors were infected into LLC-MK2 or HeLa cells. FIR protein expression level was examined by western blot with anti-FIR antibody (6B4) (Figure 2C). At least 1×10^{10} CIU of fusion gene-deficient SeV/dF/FIR virus particles were prepared at amplification for use in the experiments.

Transduction efficiency of the SeV/dF/GFP vector in various human tumor cell lines

Nine human and five murine tumor cell lines plus non-tumor cells, propagated *in vitro* were collected, transduced by SeV/dF/GFP, and examined for gene transduction efficiency. Flow cytometric analyses showed dose-dependent GFP expression, and optimal expression was obtained at a MOI of 10-100; > 90% GFP-positive tumor cell lines were detected at a MOI over 10 (Figure 3A and data not shown). Furthermore, SeV/dF/FIR, but not SeV/dF/GFP significantly suppressed HeLa cell (human cervical squamous carcinoma) growth as shown by the APOPercentage assay (Figure 3B), indicating SeV/dF/FIR suppresses tumor cell growth by apoptosis *in vivo*.

SeV/dF/FIR vector showed anti-tumor activity in the mouse xenograft model

SeV/dF/FIR, but not SeV/dF/GFP, significantly suppressed cell growth in HeLa cells (Figure 4A) and SW480 cells when analyzed by Dunnet's test for multiple comparisons (Figure 4B). Of note, xenograft tumors 2 cm in diameter disappeared completely following SeV/dF/FIR treatment, indicating that SeV/dF/FIR has immunological effects (Figure 5)[24,25].

FIR was co-immunoprecipitated with SAP155

If SeV/dF/FIR is to be tested clinically, endogenous FIR-interacting proteins should be identified to avoid unexpected side effects. For this purpose, the FIR-FLAG tag vector was transiently expressed in 293T cells and co-immunoprecipitated with anti-FLAG conjugated beads to detect FIR-binding proteins[19-23] (Table 1). As reported previously, FBP (Far upstream element-binding protein)[26,27], SAP155[28], and SRp54 (splicing factor, arginine/serine rich-12)[28] were identified as candidate FIR-binding proteins. To date, no significant side effects have been observed following SeV/dF/FIR treatment including our study[29].

SeV/dF/FIR suppressed SSA-activated c-Myc

We previously reported that the adenovirus vector encoding FIRΔexon2 (Ad-FIRΔexon2) activates not only *c-myc* transcription, but also c-Myc protein expression in HeLa cells[8]. However, the extent of c-Myc protein activation by Ad-FIRΔexon2, evaluated by western blot analysis, could not be explained solely by *c-myc* transcription activation[8]. Therefore, we hypothesized that c-Myc protein should be modified by Ad-FIRΔexon2 to be more stable. Ad-FIRΔexon2 expression leads to increased levels of c-Myc phosphorylated at Ser62 (data not shown), indicating that stable c-Myc protein accumulates in cells[30,31]. As reported previously, SAP155 siRNA inhibited FIR pre-mRNA splicing and generated FIRΔexon2[8,9]. In fact, SAP155 siRNA increased levels of c-Myc phosphorylated at Ser62 and Ad-FIRΔexon2 (Figure 6A). In other words, Ad-FIRΔexon2, which lacks the transcriptional repressor

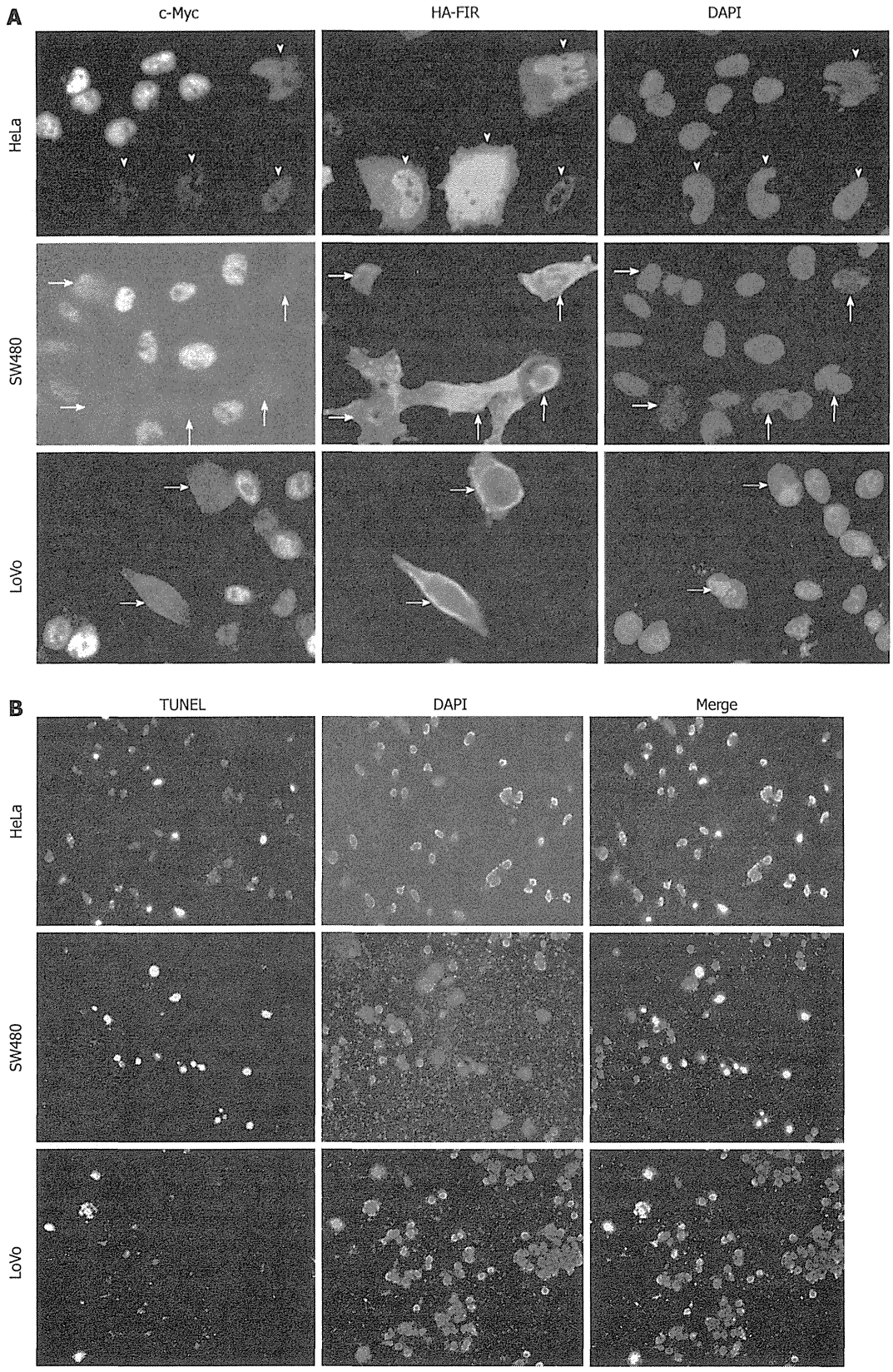

Figure 1 Far up stream element-binding protein-interacting repressor suppresses endogenous c-Myc in SW480 and LoVo cells as well as HeLa cells. A: 100 fmol of HA-FIR was transfected into the colon cancer cell lines, SW480 and LoVo cells, as well as HeLa cells (cervical squamous cell carcinoma cells) in a 6-well plate. After 48 h transfection, cells were fixed and immunostained against c-Myc (left, green) or HA (middle, red) antibodies. Arrowheads (HeLa), thick arrows (SW480) and thin arrows (LoVo) show the cells in which HA-FIR plasmids were expressed. c-Myc expression (left, green) was markedly reduced in most HA-FIR-expressing cells (middle, red) (indicated by arrowheads and arrows); B: HA-FIR transfected cells were definitively associated with apoptosis as revealed by TUNEL assay in HeLa, SW480 and LoVo cells. Nuclear DNA was stained with DAPI (right, blue). FIR: FBP Interacting Repressor; FBP: FUSE-Binding protein; FUSE: Far Upstream Element.

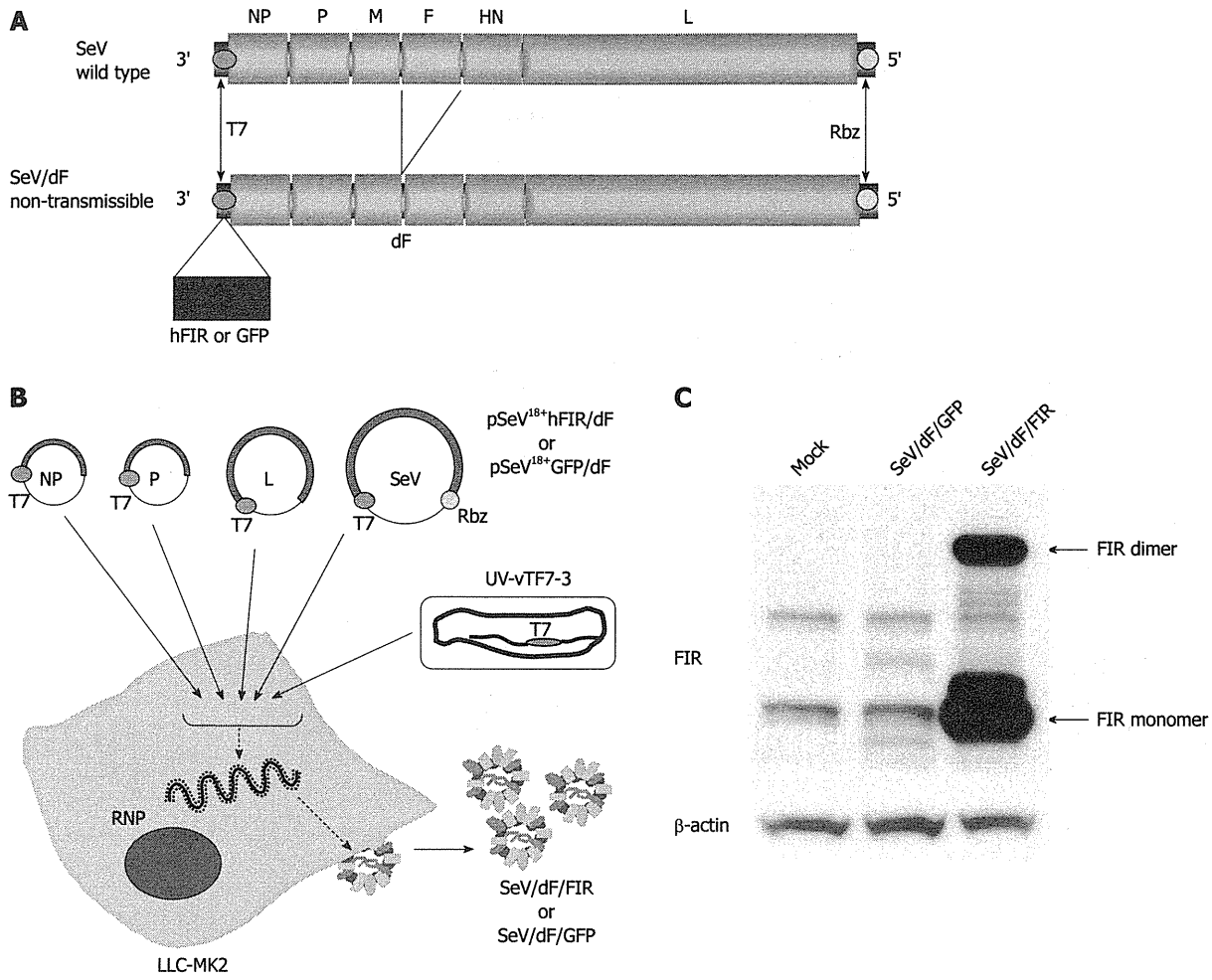

Figure 2 Structures and procedures for generating fusion gene-deficient Sendai virus/dF/far up stream element-binding protein-interacting repressor (SeV/dF/FIR) or Sendai virus/dF/green fluorescent protein vectors (SeV/dF/GFP) from Sendai virus genome RNA. A: Schematic genome structures of wild-type (SeV) and fusion gene-deficient (SeV/dF; non-transmissible) vector carrying the human FIR (*hFIR*) gene or jellyfish green fluorescent protein (GFP). The open reading frame or the *FIR* or *GFP* gene was inserted with the SeV-specific transcriptional regulatory signal sequences. T7; T7 promoter, Rbz; hepatitis delta virus ribozyme sequence; B: Schematic representation of the procedure for generating the fusion gene-deficient SeV/dF/FIR or SeV/dF/GFP. SeV/dF/FIR or SeV/dF/GFP virus particles were propagated using fusion protein-expressing packaging cells (LLC-MK2/F7/A) after preparation in LLC-MK2 cells using the four plasmids driven by a recombinant vaccinia virus expressing T7 RNA polymerase which had been inactivated with psoralen and long-wave UV light (UV-vTF7-3); C: SeV/dF/FIR virus vectors were infected into HeLa cells and whole cell proteins were extracted for western blot analysis. SeV/dF/FIR expresses FIR proteins. FIR: FBP Interacting Repressor; FBP: FUSE-Binding protein; FUSE: Far Upstream Element; SeV: Sendai virus; NP: Nucleoprotein; P: Phosphoprotein; L: The catalytic subunit of the polymerase large protein forms a ribonucleoprotein complex (RNP) vector and was transfected separately with the SeV RNA. See Materials and Methods.

domain, directly or indirectly activated *c-myc* expression not only through transcription, but also through protein level, suggesting that FIRΔexon2 acts in opposition to the repressor function by FIR[8].

In this study, the effect of SeV/dF/FIR was examined to determine whether it suppresses the increase in c-Myc after SSA treatment. SeV/dF/FIR suppressed SSA-induced c-Myc activation (Figure 6B, compare lane 2 with lane 1), but not basal c-Myc expression (Figure 6B, compare lanes 4 to 3 and 6 to 5, respectively). These results were consistent with previous reports that FIR suppresses activated, but not basal, *c-myc* transcription[6]. These observations suggest that the increase in *c-myc* by either SAP155 siRNA or SSA treatment is due to reduced FIR activity, or an increase in the ratio of FIRΔexon2/FIR in HeLa cells. Taken together, these results suggest that SeV/dF/FIR is potentially clinically applicable for cancer therapy as it counteracts SSA-activated c-Myc (Figure 6B, compare lane 2 with lane 1) as well as endogenous c-Myc (Figure 1A).

SeV/dF vector transduction

F gene-deficient SeV vectors (SeV/dF) can transduce cells in a wide range of tissues such as respiratory, nervous, muscular, epithelial and immune tissues[11,32-35]. Transduction efficiency to cell lines from various tissues was examined and compared to the adenovirus vector expressing LacZ (Ad5/LacZ) at the same MOI. The transduction efficiency of SeV/dF to those cells was even higher than that of adenovirus vector (Figure 7).

DISCUSSION

Overexpression of c-Myc has been known to promote

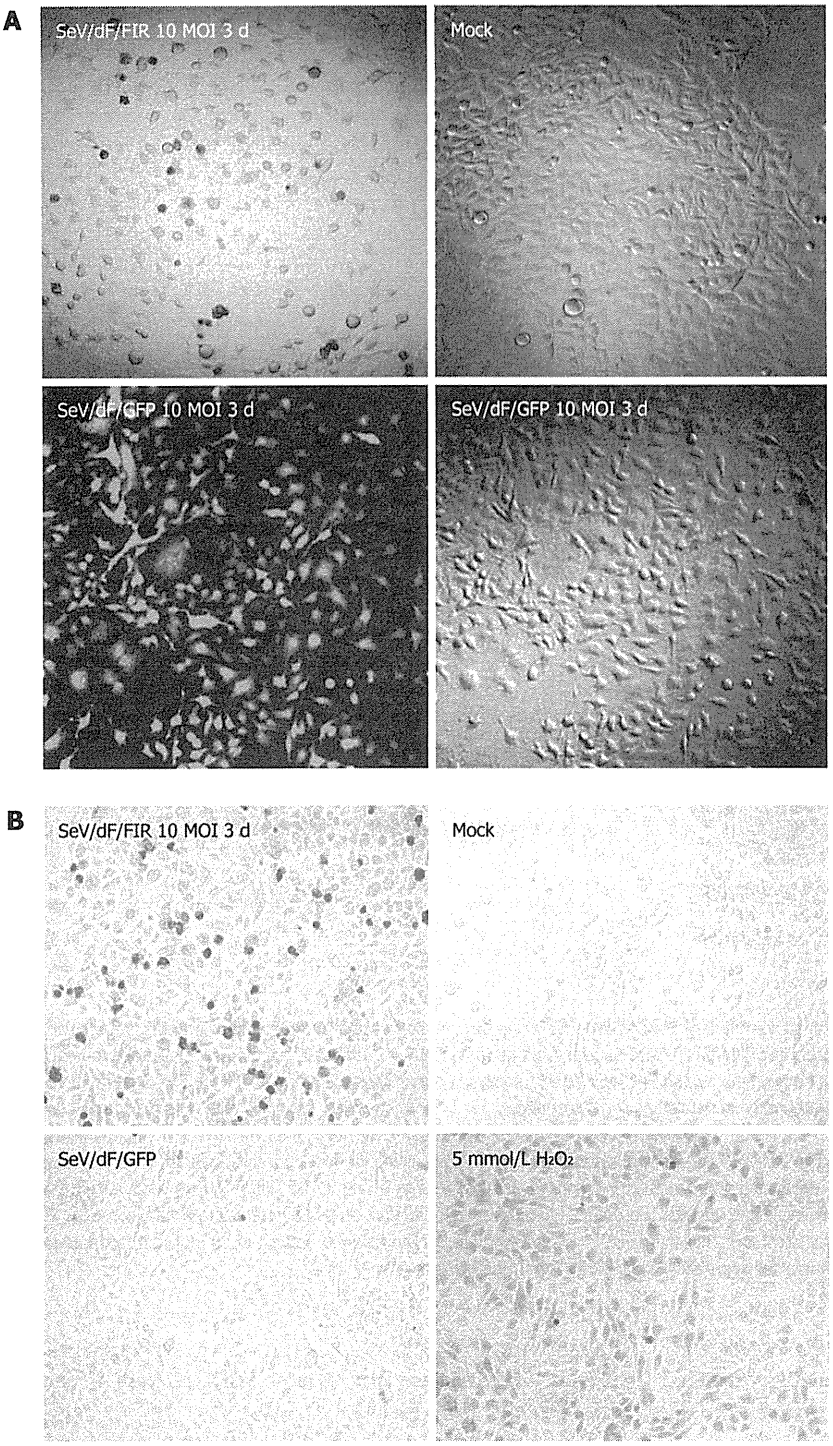

Figure 3 High efficiency of Sendai virus/dF/green fluorescent protein vectors to HeLa cells and Sendai virus/dF/green fluorescent protein vectors indicates significant cell growth inhibition with apoptosis. A: HeLa cells were infected with a 10 MOI of SeV/dF/FIR virus vector and cultured in DMEM for 3 d (72 h). The same amount of 10 MOI SeV/dF/GFP was also used to infect the control. As shown in the left lower panel, SeV/dF/GFP infected almost 100% cells (green). Under these conditions, SeV/dF/FIR significantly inhibited cell growth as shown in the left upper panel. Mock and 10 MOI SeV/dF/GFP showed no cell growth inhibition as seen in the right upper and lower panels; B: HeLa cells infected by 10 MOI SeV/dF/FIR for 3 d showed significant cell damage revealed by the APO Percentage apoptosis assay™, compared to mock or the same conditions of SeV/dF/GFP virus infected HeLa cells. 5 mmol/L H_2O_2 was used as a positive control. FIR: FBP Interacting Repressor; FBP: FUSE-Binding protein; FUSE: Far Upstream Element; SeV: Sendai virus; GFP: Green fluorescent protein; MOI: Multiplicity of infection.

cell growth, proliferation and immortalization, whereas a reduction in c-Myc induces apoptosis. The recent genetic construction of the mouse in which the expression of *c-myc* can be switched on or off *in vivo* has emphasized the significance of c-Myc expression in tumorigenesis. Ectopic *c-myc* expression in hematopoietic cells using the tetracycline regulatory system caused malignant T cell lymphomas and acute myeloid leukemia; subsequent inactivation of the transgene caused regression of established tumors[36]. These observations have provided encourage-